A critical evaluation of deterministic methods in size optimisation of reliable and cost effective standalone hybrid renewable energy systems

Alireza Maheri
Faculty of Engineering and Environment, Northumbria University, Newcastle upon Tyne, NE1 8ST, UK

alireza.maheri@northumbria.ac.uk

Abstract
Reliability of a hybrid renewable energy system (HRES) strongly depends on various uncertainties affecting the amount of power produced by the system. In the design of systems subject to uncertainties, both deterministic and nondeterministic design approaches can be adopted. In a deterministic design approach, the designer considers the presence of uncertainties and incorporates them indirectly into the design by applying safety factors. It is assumed that, by employing suitable safety factors and considering worst-case-scenarios, reliable systems can be designed. In fact, the multi-objective optimisation problem with two objectives of reliability and cost is reduced to a single-objective optimisation problem with the objective of cost only. In this paper the competence of deterministic design methods in size optimisation of reliable standalone wind-PV-battery, wind-PV-diesel and wind-PV-battery-diesel configurations is examined. For each configuration, first, using different values of safety factors, the optimal size of the system components which minimises the system cost is found deterministically. Then, for each case, using a Monte Carlo simulation, the effect of safety factors on the reliability and the cost are investigated. In performing reliability analysis, several reliability measures, namely, unmet load, blackout durations (total, maximum and average) and mean time between failures are considered. It is shown that the traditional methods of considering the effect of uncertainties in deterministic designs such as design for an autonomy period and employing safety factors have either little or unpredictable impact on the actual reliability of the designed wind-PV-battery configuration. In the case of wind-PV-diesel and wind-PV-battery-diesel configurations it is shown that, while using a high-enough margin of safety in sizing diesel generator leads to reliable systems, the optimum value for this margin of safety leading to a cost-effective system cannot be quantified without employing probabilistic methods of analysis. It is also shown that deterministic cost analysis yields inaccurate results for all of the investigated configurations.

Keywords: power reliability; design optimisation under uncertainties; hybrid renewable energy system; wind-PV-battery; wind-PV-diesel; wind-PV-battery-diesel

1 Introduction
Ideally, a standalone hybrid renewable energy system (HRES) must be as cost effective as and as reliable as a grid connected HRES or its equivalent fossil fuel power system. This makes sizing of standalone HRES a multi-objective optimisation problem with two conflicting objectives of cost and reliability. The term cost may refer to either one of the traditional parameters such as total life-span cost (TLSC), annualised cost and the levelised cost of energy (LCE) which concern investors and the end-users, or in an integrated design approach, a combination of one of the traditional cost

parameters and the life-cycle carbon foot print of the system, as the cost imposed to the environment.

Reliability of a HRES is a general term and can be represented in different ways depending on the system configuration, failure modes and failure mechanisms. Section 3 elaborates on various measures of reliability of HRES. Reliability of a HRES, irrespective of its definition, depends on various uncertainties affecting the amount of power produced by the system. Stochastic nature of renewable resources imposes a great deal of uncertainty in the system operation and the power supply. Another source of uncertainty is the stochastic demand load. The demand load is under the influence of many parameters, most of them with a level of uncertainty. For example, in case of a household demand load, the unpredictable inhabitant behaviour in energy consumption is a major source of uncertainty affecting the actual demand load. Initial sizing of the components at conceptual design phase is based on many low fidelity models, mainly due to lack of solid information on the type, make and performance of the components to be selected. This imposes some uncertainty to the system modelling and predicted power and consequently impacts the confidence in evaluation of design candidates during the design process. Another type of uncertainty which affect the cost rather than the power supply is due to uncertainty in variable part of the operating cost (e.g. fuel price in case of systems including diesel generators) and economical uncertainty during the life-span of the system (e.g. inflation and interest rates).

In design of systems subject to uncertainties both deterministic and nondeterministic design approaches are very popular. In a deterministic design approach (also called classical design), the designer is aware of the uncertainties involved in the design problem and he can quantify them to some extents. The designer considers the presence of uncertainties and incorporates them indirectly into the design by applying safety factors (e.g. load factor, margin of safety and factor of safety). In cases with known uncertainties and simple models, it is also possible to identify the worst-case-scenarios and carry out the design based on these scenarios. In many design practices a combination of safety factors and worst-case-scenarios is applied. Most of the literature on design of standalone HRES adopt this approach (for example, see [1-10]).

On the other hand, adopting a nondeterministic approach, the reliability of the system becomes directly involved in the design problem formulation, either as an objective or as a constraint, and plays a major role in design candidate assessment. All uncertainties are considered and probabilistic evaluation methods are used to evaluate the relevant reliability measures. For instance, see Roy et al [11, 12].

In this paper, through case studies, the competence of deterministic design methods in size optimisation of reliable standalone HRES is examined. The rest of the paper is structured as follows: Section 2 details the deterministic design methods for three most popular standalone HRES configurations: Renewable-Battery (RB), Renewable-Diesel (RD), and Renewable-Battery-Diesel (RBD). In Section 3, various performance assessment criteria and the probabilistic method of reliability analysis are discussed. Section 4 covers the equations used for power and cost modelling. In Section 5, deterministic design case studies are carried out and employing Monte Carlo simulation method, the reliability of the designed systems are evaluated.

2 Deterministic Design of Standalone HRES

Adopting a deterministic approach, size optimisation of standalone HRES is carried out for a worst-case-scenario, while applying a load factor on the demand load. All calculations are based on the averaged values over a period of time. The stochastic nature of demand load and renewable resources as well as the possible errors in the results due to employing low fidelity models are ignored. No reliability measure is calculated as part of the design candidate assessment. It is assumed that an educated selection of the worst-case-scenario and the load factor (a wise decision made by the designer at the beginning of the process) will lead to reliable solutions. In fact, the multi-objective optimisation problem with two objectives of reliability and cost is reduced to a single-objective optimisation problem with the objective of cost only.

In practice, normally, the size of the storage and backup/auxiliary components are determined based on a suitable worst-case-scenario to achieve a level of confidence in the expected power supply, while the remaining components are optimised for minimising the cost (i.e., TLSC or LCE). The worst-case-scenario is normally defined based on an autonomy period. After sizing the storage or backup/auxiliary components, a single-objective optimisation search can be carried out to find the optimum size of the renewable components.

2.1 Renewable with long-term battery bank storage

RB configuration, encompassing wind turbine and/or PV panels as renewable power supply and a battery bank as storage, is suitable for high penetration sites, where the availability of renewable resources (wind and/or solar irradiance) is high. In these systems, for a part of the day the power produced by the renewable resources is higher than the demand load (excess power). During this period the excess power is directed to the battery bank. The stored energy in the battery bank is used to compensate the power deficit for the rest of the day when the renewable power is insufficient to supply the demand load.

For systems of this kind, as a standard and widely used approach, first the size of the battery bank n_B is obtained for a defined worst-case-scenario. In the second step, the size of wind turbine A_{WT} and PV panel A_{PV} are obtained by solving an optimisation problem with the objective of minimising the cost subject to the constraint of having the yearly-averaged renewable power $\overline{P}_{y,R}$ greater than or equal to the yearly-averaged load $\overline{L}_y$ with a margin of safety: $\overline{P}_{y,R} \geq (1+\mathrm{MoS})\overline{L}_y$. It should be noted that here $(1+\mathrm{MoS})$ can be interpreted as the load factor. A popular worst-case-scenario is based on assuming that, for a period of time T_a, known as the autonomy period (normally in days), the daily-averaged load $\overline{L}_d$ has its maximum value $\overline{L}_d = \overline{L}_{d,max}$ and the amount of power produced by the renewable resources is zero ($P_R = 0$). Assuming that at the beginning of the autonomy period the battery bank is fully charged, the size of the battery bank that is required to cover the load for the entire of the autonomy period can be calculated. It is commonly accepted that the reliability of the designed system depends on the length of the autonomy period T_a used in sizing the battery bank and the margin of safety MoS used for sizing the renewable components. As mentioned earlier, the accuracy of this statement will be examined in Section 5.

2.2 Renewable with diesel generator as auxiliary or backup power unit

RD systems are normally used in (i) high penetration sites, in which the renewable power production is higher than the demand load all through the day and the diesel generator is used only as a backup power unit, and (ii) low/medium penetration retrofitted sites in which originally the diesel generator has been the main source of power production and renewable components have been added later to reduce the cost of energy and/or emission.

The same deterministic approach as described above can be used for sizing RD systems. That is, first the size of the diesel generator (nominal power) $P_{D,nom}$ is obtained for a defined worst-case-scenario and then the size of the renewable components is optimised for the cost. The worst-case-scenario used for RD systems is different from the scenario normally used for RB systems. In sizing the diesel generator, normally, it is assumed that the diesel generator can cover the maximum peak load with a reasonable margin of safety when the amount of power produced by renewable resources is zero. Hence, the data with the smallest available time scale is used for identifying the peak load and the required diesel nominal power $P_{D,nom}$. Using hourly-averaged data, the constraint on the required nominal diesel power becomes $P_{D,nom} \geq \left(\overline{L}_h\right)_{max}(1+MoS)$, where $\overline{L}_h$ is the hourly-averaged load. Moreover, in contrast to the deterministic method used for RB systems, for which the constraint $\overline{P}_{y,R} \geq (1+MoS)\overline{L}_y$ is required to be satisfied assuring there is enough power to supply the demand load, here, since there are two sources of power (renewable and diesel), no constraint is required to be applied on the amount of yearly-averaged produced renewable power.

It should be noted that sizing the renewable components entirely driven by the traditional cost measures (e.g. LCE) may lead to diesel-only systems. This is due to the fact that LCE produced by diesel can be less than that of renewable for regions with low renewable resources. Using a HRES for low-renewable places is not cost effective unless an integrated cost measure which includes the system carbon foot print is used. A simplified integrated design can be carried out without calculating the system carbon foot print, but instead applying a constraint on the system penetration, $w:\ w=\frac{\overline{P}_{y,R}}{\overline{L}_y} \geq w_{design}$. The imposed constraint can be justified as a means to consider the system carbon foot print in the cost analysis indirectly, as the carbon foot print of renewable components is less than of that of fossil fuelled components.

It is commonly accepted that the reliability of the designed system with respect to the power availability depends on the margin of safety MoS used for sizing the diesel generator. The accuracy of this statement will be also examined in Section 5.

2.3 Renewable with diesel generator and battery bank

RDB systems are normally used in low to medium penetration sites. Compared to RB systems, the size of the battery bank in RDB systems is smaller as the energy stored in the battery bank compensate for the marginal power deficits. The diesel generator operates only when the power deficit is high or there is not enough stored energy in the battery bank to cover the power deficit.

The same deterministic approach as described for RD systems in which the diesel generator is sized based on a worst-case-scenario can be used for these systems. However, due to the presence of a battery bank acting as storage, the worst-case-scenario defined for RBD systems is based on an averaged load instead of the maximum peak load: $P_{D,nom} = \frac{1}{T}\int_T L(1+MoS)dt$. Since, normally, the load distribution is given for typical days of different months or seasons, in defining the averaged load, T is usually taken as 1 day (the one with the highest demand load). This is equivalent to sizing the diesel for an autonomy period of $T = T_a = 1\,\text{day}$. After sizing the diesel, the minimum size of the battery bank $n_{B\min}$ must be found to make sure that the combination of diesel-battery can cover the demand load for the period of T in the case of $P_R = 0$. The size of the renewable components can be obtained through an optimisation problem with a constraint on the size of the battery bank $n_B \geq n_{B\min}$ and the optional constraint on the system penetration $w = \frac{\overline{P}_{y,R}}{\overline{L}_y} \geq w_{design}$.

3 Reliability Assessment

Performance of a standalone HRES in supplying power can be evaluated against different assessment criteria, such as unmet load, blackout duration, loss of load probability, blackout distribution and the mean-time between failures, as explained below.

3.1 Unmet Load

Unmet load, U is an availability based parameter defined as the non-served load divided by the total load of a period of time (normally one year) [7]. For a standalone HRES the unmet load is defined as:

$$U = \frac{1}{T}\int_0^T \left(1 - \frac{P_a(t)}{L(t)}\right)dt \qquad (1)$$

where, P_a and L are, respectively, the usable available power and the demand load ($0 \leq P_a \leq L$), and T is the duration of the system operation for which the performance is evaluated (normally one year). Usable available power is defined as:

$$P_a = \min\{P_{t,a}, L\} \qquad (2)$$

where, $P_{t,a}$ stands for the total available power, which is the summation of the renewable, non-renewable and stored energy.

Unmet load is dimensionless and lies between zero and one. Case $U = 0$ corresponds to a system producing enough energy whenever there is a demand. Other forms of unmet load can be also used. For example, total unmet load U_t:

$$U_t = U\int_0^T L(t)dt \qquad (3)$$

Using hourly-averaged load ($\overline{L}_h$) and hourly-averaged useable available power ($\overline{P}_h$), Equations (1) and (3) can be rewritten as

$$U = \frac{1}{8760}\sum_{i=1}^{8760}\left(1-\overline{P}_{h,a}/\overline{L}_h\right)_i \quad (4)$$

and

$$U_t = U\sum_{i=1}^{8760}\left(\overline{L}_h\right)_i \quad (5)$$

This measure is suitable when the HRES encompass a control system capable of regulating the load, for example, by cutting off the electricity supply to some part of a village. Unmet load is easy to calculate and is widely used in size optimisation of standalone HRES. However, from the end-user point of view, it does not provide tangible information.

3.2 Blackout Duration

Total blackout duration, BO_t is also an availability based parameter. In case of smaller HRES without a power supply distributor, or when the power supply distribution is not possible, for example when HRES is used to supply the electricity to a single load, an unmet load leads to blackout. In cases like this, the total blackout duration BO_t, given by Equation (6), can be used instead as a measure for the performance of the system.

$$BO_t = \int_0^T \max\left\{0, \text{sign}\left(1-\frac{P_a(t)}{L(t)}\right)\right\}dt \quad (6)$$

Sign function $\text{sign}(\varphi) = +1$ if $\varphi > 0$; $\text{sign}(\varphi) = -1$ if $\varphi < 0$; and $\text{sign}(\varphi) = 0$ if $\varphi = 0$. Using hourly-averaged data and a period of analysis of $T = 1\ \text{year} = 8760\ \text{h}$, Equation (6) can be rewritten as

$$BO_t = \sum_{i=1}^{8760}\max\left\{0, \text{sign}\left(1-\left(\overline{P}_{h,a}/\overline{L}_h\right)_i\right)\right\} \quad (7)$$

Blackout duration is superior to unmet load from the end-user point of view as it corresponds to the total duration of the system downtime (e.g. in hours) rather than to the amount of power deficit. In contrast to the unmet load, assessment of design candidates based on blackout duration allows performing customer-need driven designs.

3.3 Loss of Load Probability

Loss of load probability, LLP is defined as the proportion of time that the available power is expected to be unable to meet the demand load. Although this measure includes the term probability, in calculations no probabilistic analysis is carried out. This measure is also an availability based parameter. It is simply the blackout duration divided by the operation time:

$$LLP = \frac{1}{T}\int_0^T \max\left\{0, \text{sign}\left(1-\frac{P_a(t)}{L(t)}\right)\right\}dt \quad (8)$$

Alternatively, using hourly-averaged power and load, LLP can be represented as the ratio of the number of blackout hours to the total number of hours in a year.

$$LLP = \frac{1}{8760}\sum_{i=1}^{8760}\max\left\{0, \text{sign}\left(1-\left(\overline{P}_{h,a}/\overline{L}_h\right)_i\right)\right\} \quad (9)$$

3.4 Blackout Distribution

Another availability based parameter which has significant effect on the assessment of a HRES but rarely is being used in design and evaluation of standalone HRES is the distribution of the blackout duration. The information that can be extracted from the blackout distribution, such as the maximum blackout duration BO_{max} and the average blackout duration BO_{av}, play important role in evaluation of the system performance from the end-user point of view. For example, a total blackout duration of $BO_t = 400\,h$, can be tolerated for some applications if it is uniformly distributed throughout the year. A case like this corresponds to smaller maximum and average blackout durations. On the other hand, for a system in which most of the blackout occurs over a portion of the year only, say two months, the maximum and the average blackout duration increase. Such a system can be reasonably evaluated as unreliable for some applications. The distributions of the blackout strongly depend on the load and resource distributions, as well as the size of the system. Using blackout distribution and extracting parameters such as the maximum and the average blackout durations, more comprehensive assessment of the system performance in terms of the availability of the power supply can be carried out.

3.5 Mean Time between Failures

Mean time between failures (MTBF) can be also viewed as an availability-based parameter, if the successful system operation is defined as the case when available usable power is greater than the load $P_a > L$ and the failure is defined as blackout:

$$MTBF = \frac{1}{n_{fail}}\int_0^T \max\left\{0, \text{sign}\left(\frac{P_a(t)}{L(t)}-1\right)\right\}dt \quad (10)$$

where n_{fail} is the number of failures (the number of blackout occurrences) during period T. Using hourly-averaged quantities, $MTBF$ is defined as:

$$MTBF = \frac{\sum_{i=1}^{8760}\max\left\{0, \text{sign}\left(\left(\overline{P}_{h,a}/\overline{L}_h\right)_i-1\right)\right\}}{n_{fail}} \quad (11)$$

3.6 Reliability Analysis

Concepts such as failure rate (FR) or probability of failure (PF) are well established concepts for quantifying the reliability of renewable system in delivering a predefined function. For instance see [13-19]. Although the FR of the components and the configuration of a standalone HRES affect its reliability, the main cause of the system failure in producing enough power to supply the demand load is the stochastic nature of the renewable resources. This makes the reliability analysis of a

standalone HRES impossible without performing a complete probabilistic reliability analysis, e.g. through a Monte Carlo simulation. Monte Carlo simulation is a popular probabilistic method employed in design under uncertainty to evaluate system probability of failure for problems with multiple failure modes. The following algorithm details the reliability analysis of standalone HRES:

Given:

- $x_i = \tilde{x}_i + \hat{x}_i;\ i = 1,2,...,n_u$ the set of n_u uncertain parameters (demand load, resources and power/cost model) and their range and form of distributions. Variable $\tilde{x}_i$ is the known mean value of parameter x_i and $\hat{x}_i$ is the random variation of x_i with known distribution. For demand load and resources, x_i is a function of time: $x_i(t) = \tilde{x}_i(t) + \hat{x}_i(t)$.
- The target performance measures over a reference period of time $R_j;\ j = 1,2,...,n_p$ (e.g. $BO_t = 0$, $U_t = 0$, $MTBF = 8760$ h, etc over one year).
- Design candidate $\{A_{WT}, A_{PV}, P_{D,nom}, n_B\}$

1. Repeat n_{sim} times
   1.1. For each $x_i;\ i = 1,2,...,n_u$, select a random value $\hat{x}_i$ (a random vector $\hat{x}_i(t)$ for time dependent uncertain parameters) in the range consistent with its corresponding distribution.
      1.1.1. For each assessment criterion (target performance measures), $R_j;\ j = 1,2,...,n_p$
      1.1.2. Assess the design candidate and assign "fail" to this design candidate if the target performance measure is not met.
2. Calculate the probability of failure for this design candidate with respect to each assessment criterion using the following equation:

$$PF_j = n_{fail,j} / n_{sim};\ j = 1,2,...,n_p \quad (12)$$

In this study $n_{sim} = 10^5$ is used for all case studies.

4 Power and Cost Modelling

4.1 Power modelling and dispatch strategies

When sizing HRES components the size and therefore the characteristics of the wind turbine are not known yet. Normally, approximated power curve models $P_{WT} = P_{WT}(V_{hub})$ are used instead (see, for instance, [11, 12, 20 and 21]). To approximate a power curve four parameters, namely, rated power and cut-in, cut-out and rated wind speeds are required. These approximations are based on two assumptions: (i) the wind turbine operates at its maximum power coefficient for wind speeds below the rated wind speed, and (ii) the power curve is horizontal for wind speeds above rated wind speed. The first assumption is far from the reality particularly for constant-speed wind turbines and the second is not valid for stall-regulated wind turbines.

An alternative method, used in this paper, employs an approximated model for the power coefficient, C_P, and an estimated value for the overall efficiency of the electrical components and the gearbox, η_{EG}. The wind power produced by a wind turbine is given by:

$$P_{WT} = \frac{1}{2}\rho V_{hub}^3 A_{WT} C_P \eta_{EG} \quad (13)$$

in which ρ is the air density and V_{hub} is the wind speed at hub elevation. Power coefficient, C_P, varies with wind speed. The form of this variation depends on a variety of parameters, such as the blade design, type of wind turbine (pitch-controlled/stall-regulated, variable speed/constant speed), number of blades, etc; and it varies from one wind turbine to another. The power coefficient curve of about 60 small/medium size wind turbines up to a rated power of 500kW are selected to find an approximated model. Since standalone HRES are normally used to power relatively small demand loads (e.g. a house, off-grid villages in rural places, farms and small agricultural industries, etc.), the selected range of wind turbines serves well for our purpose. Using multiple polynomial regression in a least squares sense (see the appendix for details), the model of Equation 14 is found as the best fit with a maximum relative error of about 14%.

$$\begin{aligned} C_P = & -2.025\times10^{-7}V_{hub}^6 + 1.926\times10^{-5}V_{hub}^5 \\ & - 7.421\times10^{-4}V_{hub}^4 + 1.483\times10^{-2}V_{hub}^3 - 0.162V_{hub}^2 + 0.887V_{hub} - 1.508 \end{aligned} \quad (14)$$

Employing Equations (13) and (14) instead of the power curve approximation $P_{WT} = P_{WT}(V_{hub})$ has two advantages: firstly, we needs less parameters (only C_P model and η_{EG}) while the power curve approximation needs four parameters; and secondly, it has a known error that can be incorporated in a nondeterministic design ($C_P = (1 \pm 0.07)\tilde{C}_P$).

Given wind speed V_{ref} at elevation h_{ref}, the wind speed at the hub elevation h_{hub} can be calculated by the logarithmic law:

$$V_{hub} = V_{ref} \ln\left(\frac{h_{hub}}{z_0}\right) \Big/ \ln\left(\frac{h_{ref}}{z_0}\right) \quad (15)$$

in which z_0 is the site surface roughness length. The hub height depends on the size of the wind turbine, which is unknown prior to the design. For small to medium size wind turbines the hub height can be estimated via the rule of thumb [22]:

$$h_{hub} = \max\{h_c + R, 2R\} \quad (16)$$

where h_c is the minimum blade tip-ground clearance and R is the rotor radius.

Power produced by PV panels is given by

$$P_{PV} = IA_{PV}\eta_{PV} \quad (17)$$

in which, I stands for the solar irradiance and η_{PV} is the overall PV unit efficiency.

The power dispatch strategies for the battery bank and the diesel generator used in this study are listed in Table 1. For RBD configuration, the power stored in the battery bank is used only if it is greater than the power deficit or if the power deficit is greater than the nominal diesel power. The diesel generator, where required, operates in full load to cover the power deficit and also to charge the battery bank.

State of charge (SOC) of the battery bank at the end of period Δt is given by

$$SOC_{t+\Delta t} = SOC_t(1-\delta) + \frac{(\overline{P}_{\Delta t,R} - \overline{L}_{\Delta t})\Delta t}{n_B c_B V_B}\eta_B \quad (18.a)$$

$$SOC_{min} \le SOC_{t+\Delta t} \le SOC_{max} \quad (18.b)$$

where δ is the self-discharge rate and n_B, c_B, V_B and η_B are the number of batteries in the battery bank, unit nominal capacity, battery bank voltage and the efficiency of the battery in charging/discharging states respectively. In this equation it is assumed that the convertor efficiency is close to unity.

Table 1. The power dispatch strategies for the battery bank and the diesel generator.

	Case	Diesel Generator Power/Battery Status
Renewable-Battery	1	Excess power $\overline{P}_{\Delta t,R} - \overline{L}_{\Delta t} \geq 0$: The excess power is used to charge the battery bank $SOC_{t+\Delta t} \geq SOC_t$
	2	Power deficit less than the extractable power from the battery bank $0 \leq \overline{L}_{\Delta t} - \overline{P}_{\Delta t,R} \leq \overline{P}_{\Delta t,B,e}$: The power deficit is compensated by the battery bank $SOC_{t+\Delta t} < SOC_t$.
	3	Power deficit greater than the extractable power from the battery bank $\overline{L}_{\Delta t} - \overline{P}_{\Delta t,R} > \overline{P}_{\Delta t,B,e}$: Blackout; The battery bank is discharged to its minimum level $SOC_{t+\Delta t} = SOC_{min}$.
Renewable-Diesel	1	Excess power $\overline{P}_{\Delta t,R} - \overline{L}_{\Delta t} \geq 0$: No need for diesel generator power $\overline{P}_{\Delta t,D} = 0$.
	2	Power deficit less than the nominal power of the diesel generator $0 \leq \overline{L}_{\Delta t} - \overline{P}_{\Delta t,R} \leq P_{D,nom}$: The power deficit is compensated by the diesel generator $\overline{P}_{\Delta t,D} = \overline{L}_{\Delta t} - \overline{P}_{\Delta t,R}$.
	3	Power deficit greater than the nominal power of the diesel generator $\overline{L}_{\Delta t} - \overline{P}_{\Delta t,R} > P_{D,nom}$: Blackout; The diesel generator works at its nominal power $\overline{P}_{\Delta t,D} = P_{D,nom}$.
Renewable-Battery-Diesel	1	Excess power $\overline{P}_{\Delta t,R} - \overline{L}_{\Delta t} \geq 0$: The excess power is used to charge the battery bank $SOC_{t+\Delta t} \geq SOC_t$; No need for diesel generator power $\overline{P}_{\Delta t,D} = 0$.
	2	Power deficit less than the extractable power from the battery bank $0 \leq \overline{L}_{\Delta t} - \overline{P}_{\Delta t,R} \leq \overline{P}_{\Delta t,B,e}$: The power deficit is compensated by the battery bank $SOC_{t+\Delta t} < SOC_t$; No need for diesel generator power $\overline{P}_{\Delta t,D} = 0$.
	3	Power deficit greater than the extractable power from the battery bank but less than the nominal power of the diesel generator $\overline{P}_{\Delta t,B,e} < \overline{L}_{\Delta t} - \overline{P}_{\Delta t,R} \leq P_{D,nom}$: The diesel generator compensates the power deficit and charges the battery $\overline{P}_{\Delta t,D} = \min\left\{\overline{L}_{\Delta t} - \overline{P}_{\Delta t,R} + \overline{P}_{\Delta t,B,fc}, P_{D,nom}\right\}$; The battery bank is charged $SOC_{t+\Delta t} \geq SOC_t$.
	4	Power deficit greater than the extractable power from the battery bank and greater than the nominal power of the diesel generator but less than the summation of the two $\overline{P}_{\Delta t,B,e} \leq \overline{L}_{\Delta t} - \overline{P}_{\Delta t,R} \leq P_{D,nom} + \overline{P}_{\Delta t,B,e}$; $P_{D,nom} \leq \overline{L}_{\Delta t} - \overline{P}_{\Delta t,R} \leq P_{D,nom} + \overline{P}_{\Delta t,B,e}$: Both the diesel generator and the battery bank compensate the power deficit; The diesel generator works at its nominal power $\overline{P}_{\Delta t,D} = P_{D,nom}$; The battery bank is discharged $SOC_{t+\Delta t} < SOC_t$.
	5	Power deficit greater than the summation of the extractable power from the battery bank and the nominal power of the diesel generator $\overline{L}_{\Delta t} - \overline{P}_{\Delta t,R} > P_{D,nom} + \overline{P}_{\Delta t,B,e}$: Blackout; The diesel generator works at its nominal power $\overline{P}_{\Delta t,D} = P_{D,nom}$; The battery bank is discharged to its minimum level $SOC_{t+\Delta t} = SOC_{min}$.

The required power for reaching the SOC of the battery bank to its maximum value, $\overline{P}_{\Delta t,B,fc}$, can be calculated by the following equation in which η_B is the charging efficiency:

$$\overline{P}_{\Delta t,B,fc} = \frac{(SOC_{max} - SOC_t) n_B c_B V_B}{\Delta t \eta_B} \quad (19)$$

The extractable power stored in the battery bank, $\overline{P}_{\Delta t,B,e}$, can be calculated by the following equation in which η_B is the discharging efficiency:

$$\overline{P}_{\Delta t,B,e} = \frac{(SOC_t - SOC_{min}) n_B c_B V_B \eta_B}{\Delta t} \quad (20)$$

The number of required batteries to supply the power for the autonomy period T_a is given by:

$$n_{B,a} = \left\lceil \frac{T_a \overline{L}_{d,max} (1 + MoS)}{(SOC_{max} - SOC_{min}) c_B V_B \eta_B} \right\rceil \quad (21)$$

in which η_B is the discharging efficiency.

4.2 Cost modelling

TLSC analysis considers all costs over the life-span of the system. These costs are then discounted to a base year using present value analysis. Assuming there is no escalation in the price of the components, the formula for calculating the present value of TLSC is as follows:

$$C_t = \sum_{j=0}^{N_S} \frac{C_j}{(1+d)^j} \quad (22)$$

where N_S is the life-span of the system, C_t is the present value of TLSC, d is the annual discount rate, and C_j is the cost in year j including capital cost C_c, fixed operation and maintenance costs $C_{O\&M,F}$, variable operation and maintenance costs $C_{O\&M,V}$, and the replacement cost C_r. Case $j = 0$ represents the beginning of the life-span with its corresponding cost C_0, standing for the capital cost only.

The capital cost of the system (including installation cost) is given by:

$$C_c = \sum_{comp} C_{u,comp} S_{comp} (1 + \alpha_{ins,comp}) \quad (23)$$

in which S is the size of the component, C_u is the unit cost and α_{ins} is the installation cost as a fraction of the total cost of the component. Cost estimation at the conceptual design phase of HRES can be based on either cost per unit of nominal power production or cost per unit of size. To be consistent with the power models used in Section 4.1, for wind turbine and PV array the cost per unit size is used, whilst for the diesel generator and the batteries the cost per nominal power/capacity is used.

The O&M cost includes fixed and variable parts:

$$C_{O\&M} = \sum_{comp} C_{O\&M,F,comp} + \sum_{comp} C_{O\&M,V,comp} \quad (24)$$

The fixed part can be represented by

$$C_{O\&M,F,comp} = \alpha_{O\&M,comp} C_{c,comp} \quad (25)$$

The variable part of the O&M cost for wind turbine, PV and battery bank is zero. Using hourly-averaged data, the annual variable part of the O&M cost for diesel generator (the cost of consumed fuel) is given by [23]:

$$C_{O\&M,V,D} = \frac{0.246 \sum_{i=1}^{8760} \overline{P}_{h,D_i} + 0.08145 P_{D,nom} T_D}{1000} C_{fuel} \quad (26)$$

where T_D is the total number of hours that the diesel generator operates, $\overline{P}_{h,D}$ is the hourly-averaged diesel power and C_{fuel} is the fuel price.

For each component the replacement cost is given by:

$$C_r = \sum_{comp} n_{r,comp} C_{c,comp} \quad (27)$$

where n_r is the number of replacements during the life-span of the system. Having the nominal life of system (N_S), wind turbine ($N_{nom,WT}$) and PV panel ($N_{nom,PV}$) in years and the nominal life of diesel generator $N_{nom,D}$ in hours of operation, the following equations can be used to find the number of replacements of these components:

$$n_{r,comp} = \left[\frac{N_S}{N_{nom,comp}} \right] \quad \text{for wind turbine and PV panel} \quad (28)$$

$$n_{r,D} = \left[\frac{N_S T_D}{N_{nom,D}} \right] \quad \text{for diesel generator} \quad (29)$$

For the battery bank, the number of replacements depends on the number and depth of discharges DOD as well as $N_{nom,B}$ the nominal life span of the batteries:

$$n_{r,B} = \left[\max \left\{ \frac{N_S}{N_{nom,B}}, \frac{N_S}{N_{eq,B}} \right\} \right] \quad (30)$$

Having the number and depth of discharges, employing rain-flow counting method the equivalent life $N_{eq,B}$ can be calculated as:

$$N_{eq,B} = \frac{1}{\sum_{i=1}^{n_d} \frac{1}{n_{cycle\ to\ fail_i}}} \tag{31}$$

where n_d is the number of the charge-discharge cycles of the battery bank per year, $n_{cycle\ to\ fail_i}$ is the equivalent number of cycles to fail corresponding to DOD_i. Using the battery equivalent full cycles data reported in [24], the equivalent number of cycles to fail can be correlated to the DOD by

$$n_{cycle\ to\ fail_i} = 540.1 DOD_i^{-0.991} \tag{32}$$

Table 2 summarises the values used for the parameters appeared in Equations (23) to (26) and (28) to (30):

Table 2. Cost modelling parameters [23, 24].

	Wind turbine	PV panel	Battery bank	Diesel generator
S	Rotor area $A_{WT}(m^2)$	Panel area $A_{PV}(m^2)$	Capacity $n_B c_B(Ah)$	Nominal power $P_{D,nom}(W)$
C_u	$480\$/m^2$	$830\$/m^2$	$1.5\$/Ah$	$0.4\$/W_{nom}$
α_{ins}	0.2	0.4	0	0
$\alpha_{O\&M}$	0.03	0.01	0.01	0.15
N_{nom}	20 years	20 years	4 years	15000 hours
$C_{O\&M,V}$	0	0	0	$C_{fuel} = 1\$/l$ (as in Eq. (26))

TLSC is an important parameter which imposes a hard constraint in the design problem, affecting the configuration and the overall size of the designed HRES. LCE, on the other hand, allows alternatives to be compared when different scales of operation and investment exist. For systems with constant annual output over the life-span of the system LCE, C_l, can be calculated as follows:

$$C_l = \frac{C_a}{P_t} \tag{33}$$

where P_t denotes the annual energy output and C_a stands for the annualised cost, given by [23]:

$$C_a = C_t UCRF \tag{34}$$

The uniform capital recovery factor $UCRF$ is given by:

$$\mathrm{UCRF} = \frac{d(1+d)^{N_s}}{(1+d)^{N_s}-1} \tag{35}$$

It should be noted that the power produced by a standalone HRES excess to the demand load and, where applicable, charging the batteries is dumped. Therefore, in Equation (33), the usable amount of produced energy should be used instead of the system total energy output, P_t. Using hourly-averaged values for the demand load and renewable resources, LCE for a standalone HRES can be calculated as follows:

$$C_l = \frac{C_a}{\sum_{j=1}^{8760} \min\left\{\overline{P}_h, \left(\overline{L}_h + \overline{P}_{h,B,Charg}\right)\right\}_j} \tag{36}$$

in which $\overline{P}_h$ and $\overline{L}_h$ are, respectively, the hourly-averaged power and demand load and $\overline{P}_{h,B,Charg}$ stands for the hourly-averaged power used to charge the battery bank.

Cost analysis can be performed using either current or constant dollar cash flows. A current dollar analysis requires the use of a nominal discount rate (which includes the effect of inflation) and a constant dollar analysis requires the use of a real discount rate (excluding inflation). Discount rates are related to inflation rate with the following formula [25]:

$$d_{real} = \frac{1+d_{nom}}{1+i} - 1 \tag{37}$$

where i is the inflation rate and d_{nom} and d_{real} are the nominal and real discount rates respectively. The choice of real or nominal LCE depends on the purpose of the analysis. Most short-term studies are shown in current dollars, whereas long-term studies are frequently computed in constant dollars. It should be noted that, regardless of the method chosen, the most cost effective alternative will not change as long as all design candidates are evaluated using the same method [25]. In this study all cost analyses are based on constant-dollar cash flows.

5 Case studies

In deterministic design methods we do not evaluate the probability of failure and the actual reliability of the system is unknown to the designer. However, it is assumed (hoped) that, using safety factors and/or carrying out the design based on worst-case-scenarios, the ideal performance targets with negligible probability of failure will be achieved (for example, design for an autonomy period of $T_a = 3$ days would lead to a reliable design solution with zero unmet load: $(PF)_{U=0} \approx 0$). In this section, using deterministic design methods, size of components in standalone HRES with different configurations are optimised. For each configuration a variety of safety factors and autonomy periods is used. For each optimal design solution a Monte Carlo simulation is also performed to find the probability of failure of each of the performance assessment criteria.

In this study, only uncertainties in resources (wind speed and solar irradiance), demand load and modelling (wind turbine power coefficient and PV array efficiency) are considered. Since the aim of this study is to investigate the reliability of the results of deterministic size optimisation, a conservative approach in selecting uncertainties is adopted to ensure fair cases are considered for this purpose:

- The uncertainty in the cost analysis is intentionally neglected in this study. This allows to investigate the effect of uncertainties in renewable resources, power modelling and the demand load on the system cost as well as the reliability of power supply.
- The most conservative form of distribution is selected. Using deterministic methods for sizeing systems subject to uncertainties with uniform distribution is more likely to leads to relaible solutions, $(\mathrm{PF})_{U=0}=0$, with the price of over sizing. It should be noted that uniform distribution is not a realistic form of distriibution for wind speed, solar irradiance and the demand load.
- Unless precisely known (i.e. C_p model), low levels of uncertainties are selected. For example, the uncertainty in wind speed used in this study is taken as 30% for "hourly" averaged wind speed which is significantly lower than the 11% to 30% uncertainty in "yearly" averaged wind speed reported in [26]. Since solar irradiance is more predictable compared to wind speed the uncertainty is limited to only 10%. Uncertainty in the demand load is also limited to 20% which is a low level of uncertainty for domestic loads. A very low level of uncertainty of 10% is also considered for the PV array efficiency. PV array efficiency depends on the type of PV (varying between about 12% to about 16% for newly developed PV cells) as well as the working condition (e.g. accumulated dust can reduce the efficiency as large as 33% after one month of operation [27]). Table 3 summarises the uncertainties, whereby δ represents the variation range as a fraction of the mean value.

Table 3. Uncertainties in resources, demand load and modelling.

Parameter/Model	Distribution
Wind speed	Uniform ($\delta=\pm0.15$)
Solar irradiance	Uniform ($\delta=\pm0.05$)
Demand load	Uniform ($\delta=\pm0.10$)
C_p model	Uniform ($\delta=\pm0.07$)
PV array efficiency	Uniform ($\delta=\pm0.05$)

The hourly-averaged wind speed, solar irradiance and demand load are adopted from [28] and shown in the appendix.

A genetic algorithm (GA) was developed to find the optimal size of components. Special care has been made in design of reproduction operators for this GA. Figure 1 shows a typical solution space obtained using an exhaustive search with a uniform fine grid. As it can be observed, although the design space is uniform, the solution space is clustered with multiple local optima, which can impact the search performance of an ordinary GA. This property of the solution space has been taken into account in design of the mutation operator of the developed GA. In order to increase the exploratory behaviour of the GA, avoiding stagnation in local optima, a high mutation rate is used. However, to reduce the negative effect of using a high mutation rate on exploitation of the design

space, a dynamic mutation operator combined with a mixed parent selection strategy have been used. At earlier generations, identified by $\text{fit}_{av}/\text{fit}_{max} \le 0.9$ (the ratio of the average fitness of the population fit_{av} and the fitness of the best individual in the population fit_{max}), the GA explores the design space towards finding the cluster of the global optima by using a high mutation rate ($P_m = 0.7$) and a random parent selection strategy (irrespective of the individual fitness). At latest generations ($\text{fit}_{av}/\text{fit}_{max} > 0.9$) when the GA has found the cluster of the global optima, the algorithm exploits the design space towards finding the global optima itself by adopting a parent selection based on the individual fitness. In this stage still a high mutation rate is used but the mutation effect is limited. The random perturbation of the i-th design variable x_i is selected from a shrinking interval $I_{i,m}$:

$$x_{i,m} = x_{i,l} + \delta x_i \quad ; \delta x_i \in I_{i,m} = \left(1 - \frac{\text{fit}_{av}}{\text{fit}_{max}}\right)\left(x_{i,u} - x_{i,l}\right) \tag{38}$$

in which, $x_{i,m}$, $x_{i,l}$, $x_{i,u}$ and δx_i are, respectively, the mutated value, the lower limit, the upper limit and the random perturbation of design variable x_i, and $I_{i,m}$ is the mutation interval. This is aimed at a refine search in the vicinity of the global optima. Fitness is defined based on LCE:

$$\text{fit} = 1/C_l \tag{39}$$

In this algorithm an arithmetic crossover operator is used. The infeasible solutions are defined as those with nonzero total blackout duration and are rejected on creation. The algorithm terminates when $\text{fit}_{max} - \text{fit}_{av} \le 1\times10^{-5}$.

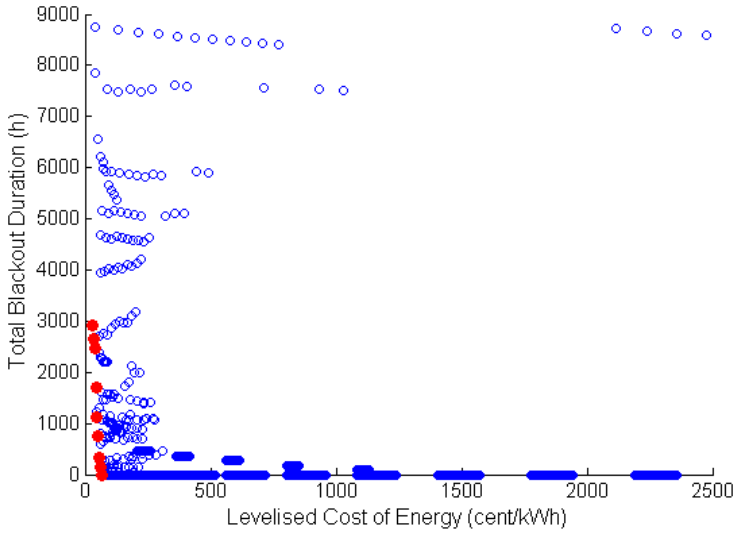

Figure 1-A typical solution space obtained using an exhaustive search over a fine uniform grid. Blue hollow circles represent solutions and red solid circles represent the Pareto front solutions.

The developed GA searches for the optimal size of components over a bounded search space: wind turbine rotor radius is either zero (representing the case of no wind turbine in the HRES configuration) or is a real number between $R_{WT,l} = 2\text{m}$ and the upper limit $R_{WT,u}$ given by Equation

(40). The upper limit can be estimated by assuming that the wind turbine is capable of producing the required renewable power to supply the demand load by its own. It is estimated using the maximum daily-averaged load and the minimum daily-averaged wind power. In this study, the minimum daily-averaged wind power is calculated at a hub elevation of $h_0 = 12\text{m}$ using a conservative value of $C_{P_0} = 0.2$ for the power coefficient, as follows:

$$R_{WT,u} = \sqrt{\frac{2\overline{L}_{d,max}}{\pi\rho C_{P_0}\left(\overline{V}_{d,min}\right)^3_{h=h_o}}} \tag{40}$$

Adopting the same approach for PV size limits, the PV panel area is either zero (representing the case of no PV panel in the HRES configuration) or is an integer number between $A_{PV,l} = 4\text{m}^2$ and the upper limit $A_{PV,u}$ defined as:

$$A_{PV,u} = \frac{\overline{L}_{d,max}}{\overline{I}_{d,min}\eta_{PV}} \tag{41}$$

In this study, where applicable, $24\text{V} - 40\text{Ah}$ lead-acid batteries have been used (self-discharge rate $\delta = 0.2\%, \eta_B = 0.9$ in charging state (independent of the charging current) and $\eta_B = 1$ in discharging state). It is also assumed that $SOC_{min} = 0.1$ and $SOC_{max} = 1$. Other parameters are as follows: air density $\rho = 1.225\text{kg/m}^3$; wind turbine electrical and gearbox efficiency $\eta_{EG} = 0.9$; surface roughness length $z_0 = 0.03\text{m}$; minimum blade tip-ground clearance $h_c = 8\text{m}$; overall PV unit efficiency $\eta_{PV} = 12\%$; the life-span of the system $N = 20$ years and the real discount rate $d_{real} = 4\%$.

5.1 Case Study 1: Wind-PV-Battery Configuration

Using deterministic optimal sizing method explained in Section 2.1, for different autonomy periods and margins of safety the optimal size of the system components are obtained and presented in Table 4. The last row of this table includes the results of optimisation without considering a margin of safety or an autonomy period, in which the size of the battery bank is determined along with the other design variables.

Table 4. RB configuration: Results of the deterministic optimal design.

Design Case	Battery bank sized based on T_a and MoS			No. of batteries	Wind turbine rotor radius (m) [rated power (kW)]	PV panel area (m^2) [nominal pick power (kWp)]	Penetration (%)	TLSC ($)	LCE (cent/kWh)
	T_a (days)	MoS(%)	$T_a(1+\text{MoS})$						
D1	1	20	1.2	146	9.7 [117]	12 [1.0]	351	289,500	50.0
D2	3	20	3.6	428	9.5 [112	25 [2.1]	341	364,860	63.0
D3	10	20	12	1460	10.1 [127]	0 [0]	380	599,730	103.6
D4	1	100	2	244	10.0 [125]	0 [0]	371	311,540	53.8
D5	3	100	6	730	9.8 [120]	11 [0.9]	359	429,110	74.1
D6	10	100	20	2432	10.3 [132]	0 [0]	398	836,400	144.5
D7	1	200	3	366	10.0 [125]	0 [0]	371	339,940	58.7
D8	3	200	9	1096	10.1 [127]	0 [0]	380	515,000	89
D9	10	200	30	3648	10.4 [135]	0 [0]	408	1,124,750	194.3
D10	Battery bank size optimised for cost			70	9.7 [117]	12 [1.0]	351	271,810	47.0

In this table and Tables 6 and 8 of Sections 5.2 and 5.3, the wind turbine rated power is calculated as the maximum of the power obtained using Equation 13 for wind speeds between 3 and 25 m/s. PV nominal pick power is calculated using Equation 17 based on standard test condition solar irradiance of 1000W/m².

Figure 2 shows TLSC and LCE of the designed systems versus the overall safety factor $T_a(1+\text{MoS})$ used for sizing the storage. This figure shows that TLSC and LCE are almost linearly proportional to $T_a(1+\text{MoS})$. This behaviour was expected since, according to Equation (21), the size of the storage is proportional to $T_a(1+\text{MoS})$ and the battery bank has a major contribution in the overall cost of the system. Beside the significant effect of the safety factor $T_a(1+\text{MoS})$ on the size of the storage and consequently cost of the system, this parameter also affects the optimum size of the renewable components as well as the system configuration (i.e. the optimal configuration in designs D3, D4 and D6-D9 do not include PV panel).

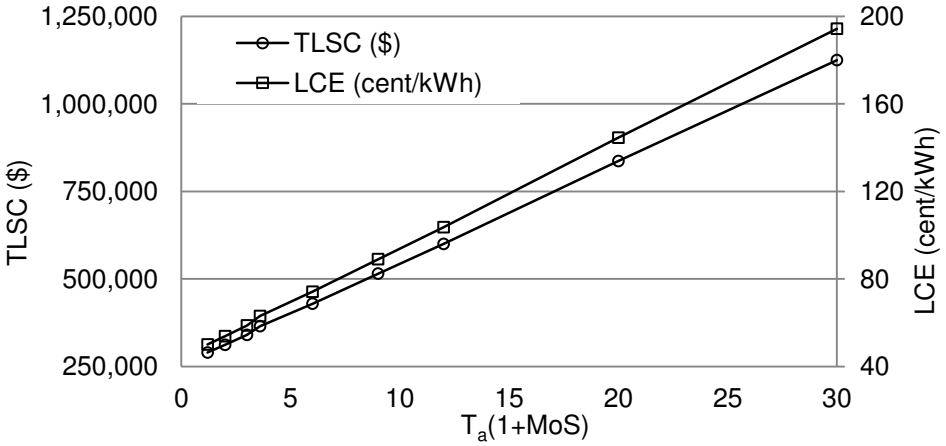

Figure 2-RB configuration: Cost versus $T_a(1+\mathrm{MoS})$.

For each design case, a Monte Carlo simulation is carried out to quantify the probability of failure of the system with respect to three system reliability measures which are expected to be achieved by using T_a and MoS in a deterministic design. The reliability measures which are considered are $U_t = 0$, $BO_t = 0$ and $\mathrm{MTBF} = 8760\mathrm{h}$. These goal values represent a reliable system in supplying the power when required. Extending the Monte Carlo simulation for cost analysis, the probability of failure in achieving a cost less than or equal to the calculated cost within a deterministic design ($C_l \le C_{l,\mathrm{det}}$) is also calculated. These results are shown in the second and third columns of Table 5. Some system performance characteristics at 99% level of confidence (LOC), equivalent to a probability of failure of $\mathrm{PF} = 1\%$, are also extracted from the results of the Monte Carlo simulation and are presented in this table.

Table 5. RB configuration: Probability of failure of design cases with respect to the reliability and cost criteria.

Design Case	Probability of Failure (%)		System performance characteristics @ 99% LOC (PF=1%)					
	$U_t = 0$ $BO_t = 0$ $\mathrm{MTBF} = 8760$	$C_l \le C_{l,\mathrm{det}}$	BO_t (h)	BO_{max} (h)	BO_{av} (h)	U_t (kWh)	MTBF (h)	C_l (cent/kWh)
D1	40.2	68.4	20	5	3	59.5	960	50.2
D2	6.7	72.8	8	4	2.5	19.9	2190	63.2
D3	8.3	68.7	11	4	3	29.5	1750	114.3
D4	1.5	65.2	4	3	2	6.0	4390	53.9
D5	9.9	70.0	11	3	2.6	31.4	1470	79.5
D6	0.3	82.2	1	0.5	0.2	0.2	8750	162.5
D7	2.4	70.4	4	3	2.5	11.5	2940	58.8
D8	1.1	29.9	2	2	1.5	3.2	4400	96.7
D9	3.8	99.9	6	4	2.5	16.6	2910	246.1
D10	100	100	107	9	2	297.4	150	47.7

Comparing the probability of failure with respect to the expected reliability measures ($U_t = 0$, $BO_t = 0$ and $\mathrm{MTBF} = 8760\mathrm{h}$) and expected cost ($C_l \le C_{l,\mathrm{det}}$) of designs D1 to D9 with design D10

(in which the battery bank is sized along with other design variables), it is evident that using safety factor $T_a(1+\text{MoS})$ in sizing the storage enhances the reliability of the system to some extents. In order to quantify this effect, the probability of failure of the system with respect to the expected reliability measures and cost versus $T_a(1+\text{MoS})$ are shown in Figure 3. It can be observed that (i) irrespective of the length of the autonomy period and the margin of safety, high probability of failure in either of the expected reliability or cost or both is expected, and (ii) while $T_a(1+\text{MoS})$ directly affects the size of the storage and consequently the cost of the system, there is no predictable pattern representing the effect of this parameter on the reliability of the system. For example, comparing designs D4 and D9, while the size of the storage and the cost of design D9 are, respectively, 15 times and 3.6 times of those of design D4, this design is less reliable than design D4 in supplying power. Considering D3 and D9, one can conclude that large battery banks, surprisingly, may lead to less reliable systems, if not accompanied by the right size for renewable components (e.g. in case of D6). This behaviour is due to significant loss of renewable energy in charging larger battery banks (re-simulating D9 with a charging efficiency of 100% instead of 90% leads to a probability of failure of zero for this design).

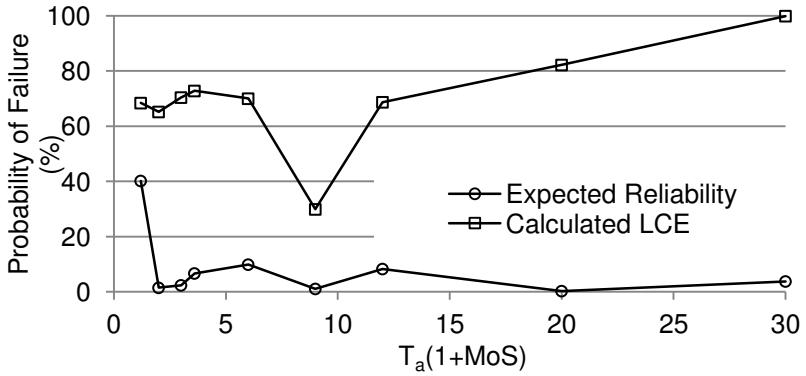

Figure 3-RB configuration: Probability of failure of the system with respect to the expected reliability and cost criteria versus $T_a(1+\text{MoS})$

Figure (4) to (5) show the system reliability characteristics (BO_t , BO_{max} , BO_{av}, U_t and $MTBF$) at 99% LOC. For all of these reliability measures, more or less the same unpredictable pattern against $T_a(1+\text{MoS})$ can be observed.

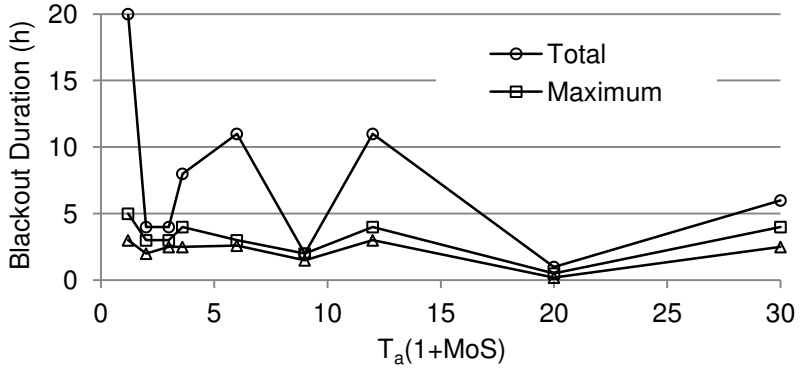

Figure 4-RB configuration: Blackout duration at 99% LOC versus $T_a(1+\text{MoS})$

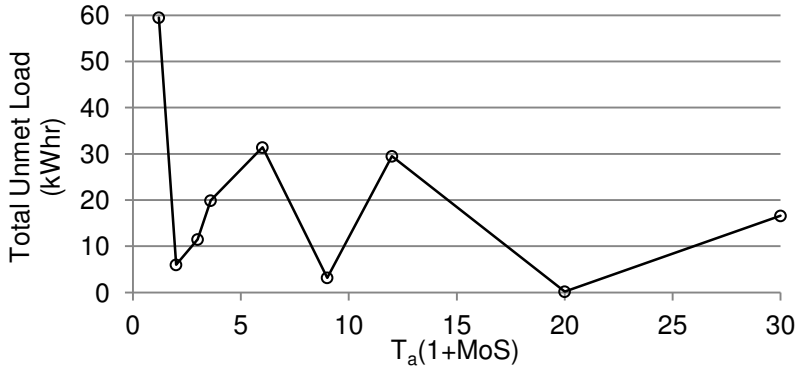

Figure 5-RB configuration: Total unmet load at 99% LOC versus $T_a(1+\text{MoS})$

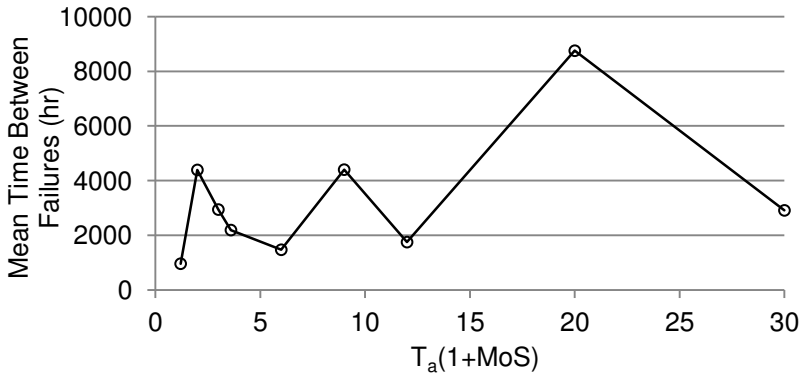

Figure 6-RB configuration: MTBF at 99% LOC versus $T_a(1+\text{MoS})$

Figure (7) shows the solution space for designs D1 to D10 in LCE-total blackout duration plane, both calculated at 99% LOC. As it can be observed only designs D1, D4, D6, D9 and D10 (marked by solid circles) are Pareto solutions. Having in mind that LCE is proportional to the overall safety factor $T_a(1+\text{MoS})$, this figure confirms that there is no predictable correlation between the overall safety factor $T_a(1+\text{MoS})$ and the reliability of the system and challenges the suitability of this parameter in design of reliable RB systems.

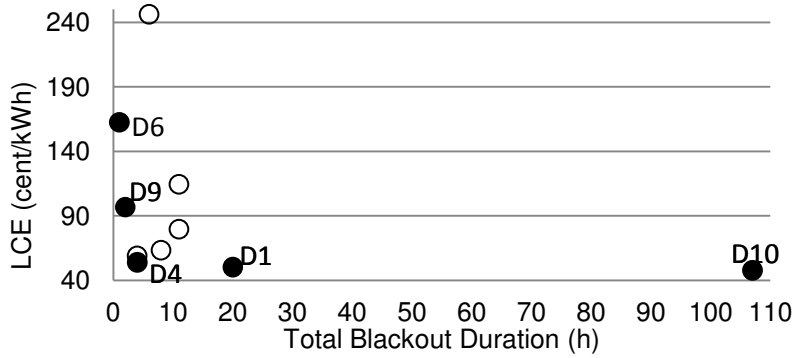

Figure 7-RB configuration: Solution space for design cases D1 to D10

Figure 8 compares LCE calculated via deterministic optimisation with the actual LCE at 99% LOC obtained by Monte Carlo simulation. The deviation between the two curves becomes more significant as the size of the storage increases. That is, as the size of the storage increases, the system is more likely to fail at producing energy at the cost predicted by deterministic methods. For example, design D6 ($T_a(1+\text{MoS}) = 20$), which is the most reliable design in terms of the reliability

of the power supply, will not produce energy at a levelised cost of 144.5 cent/kWh (calculated via a deterministic method) but at a levelised cost of 162.5 cent/kWh instead. This challenges the validity of the results of deterministic optimisation for the objective of cost as well.

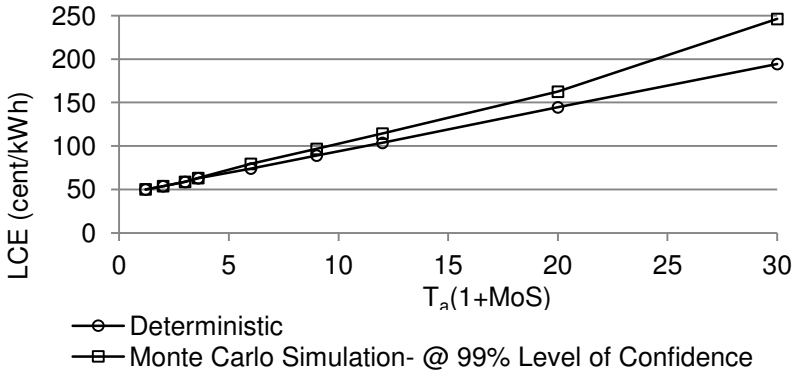

Figure 8-RB configuration: Levelised cost of energy calculated based on deterministic optimisation and the levelised cost of energy obtained by Monte Carlo simulation at 99% LOC.

With reference to Table 5, comparing designs D3 ($T_a(1+\text{MoS})=12$) with D5 ($T_a(1+\text{MoS})=6$), the advantages of using the blackout distribution instead of the unmet load can be explained. Since the unmet load for design D3 is less than the unmet load in design D5 (29.5 versus 31.4 kWh), one can conclude that design D3 is more reliable in supplying power. However, comparing the average and maximum blackout durations of design D3 to design D5 (respectively, 2.6 versus 3 and 3 versus 4), from the end-user point of view design D5 is preferred to design D3 as the domestic end-users clearly prefer shorter blackout durations.

5.2 Case Study 2: Wind-PV-Diesel Configuration

For different margins of safety the optimal size of the system components are obtained and presented in Table (6). The last row of this table includes the results of optimisation without considering a margin of safety, where the size of the diesel generator is determined along with the other design variables.

Table 6. RD configuration: Results of the deterministic optimal design.

Design Case	Diesel generator sized based on MoS MoS(%)	Wind turbine rotor radius (m) [rated power (kW)]	PV panel area (m^2) [nominal pick power (kWp)]	Diesel nominal power (kW)	Penetration (%)	TLSC ($)	LCE (cent/kWh)
D11	0	6.3 [49]	0 [0]	15.0	126	239,200	41.3
D12	20	7 [61]	0 [0]	18.0	160	255,720	44.2
D13	50	7 [61]	0 [0]	22.5	160	279,450	48.3
D14	100	7.9 [78]	0 [0]	30.0	209	313,020	54.1
D15	200	8.1 [82]	0 [0]	45.0	221	373,980	64.6
D16	Diesel generator optimised for cost	6.3 [49]	0 [0]	14.2	126	234,150	40.4

Figure 9 shows the system cost and LCE versus the margin of safety used in sizing of the diesel generator. Comparing Figures 9 and 2, the same behaviour as in RB configuration is observed here, but for a different reason. In RB configuration the battery bank has a major contribution in the overall cost of the system, while in RD configuration the share of the cost of the diesel generator is much less. The reason for observing the same behaviour can be explained as follows. As the nominal size of the diesel generator increases, the time at which the generator operates at its nominal power and consequently its highest efficiency decrease. This makes producing power less cost effective compared to the renewable power.

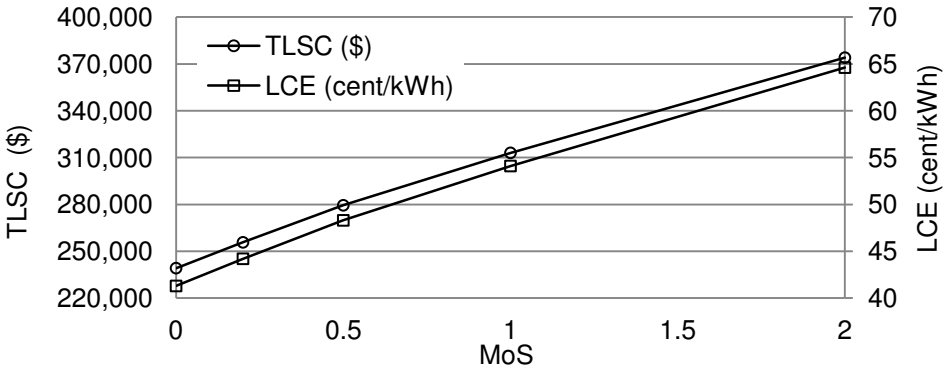

Figure 9- RD configuration: Cost versus MoS .

Similar to Case Study 1, for each design case, a Monte Carlo simulation is carried out to quantify the probability of failure of the system with respect to the system reliability measures as well as the cost. The system performance characteristics at 99% LOC are also extracted from the results of the Monte Carlo simulation and are presented in Table 7.

Probability of failure of the system with respect to the expected reliability measures and cost versus MoS are shown in Figure 10. It can be observed that for this configuration MoS serves well as a mean of designing reliable RD systems in supplying power via deterministic design methods. Obviously as the level of uncertainties in resources, demand and modelling increases larger MoS is required. On the other hand, according to this figure, irrespective of the value of the MoS used, the predicted costs via deterministic methods are not reliable (100% probability of failure of $C_l \leq C_{l,det}$ for all cases).

Table 7. RD configuration: Probability of failure of design cases with respect to reliability and cost criteria.

Design Case	Probability of Failure (%)		System performance characteristics @ 99% LOC (PF=1%)					
	$U_t = 0$ $BO_t = 0$ $MTBF = 8760$	$C_l \le C_{l,det}$	BO_t (h)	BO_{max} (h)	BO_{av} (h)	U_t (kWh)	MTBF (h)	C_l (cent/kWh)
D11	100	100	29	1	1	4.1	310	42.8
D12	0	100	0	0	0	0	8760	45.7
D13	0	100	0	0	0	0	8760	50
D14	0	100	0	0	0	0	8760	56.5
D15	0	100	0	0	0	0	8760	68.6
D16	100	100	55	1	1	13.9	160	41.9

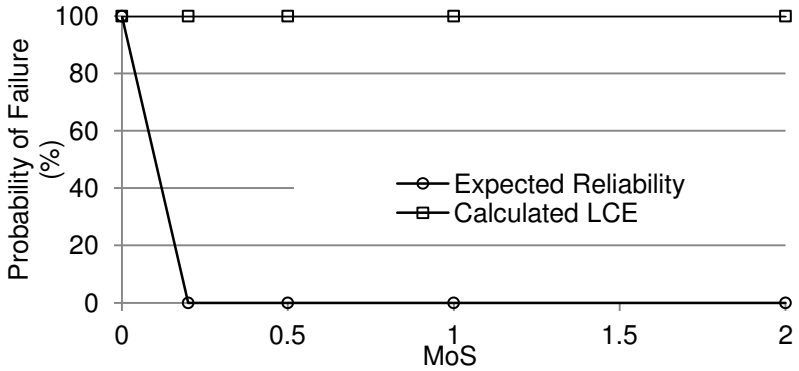

Figure 10-RD configuration: Probability of failure of the system with respect to the expected reliability and cost criteria versus MoS .

Figure 11 compares the deterministically calculated LCE with the LCE at 99% LOC obtained by Monte Carlo simulation. The deviation between the two curves becomes more significant as the size of the diesel generator increases. That is, as MoS (and consequently the size of the diesel generator) increases, the system is more likely to fail at producing energy at the predicted cost by deterministic methods. This, challenges the validity of the results of deterministic optimisation for the objective of cost for this configuration too.

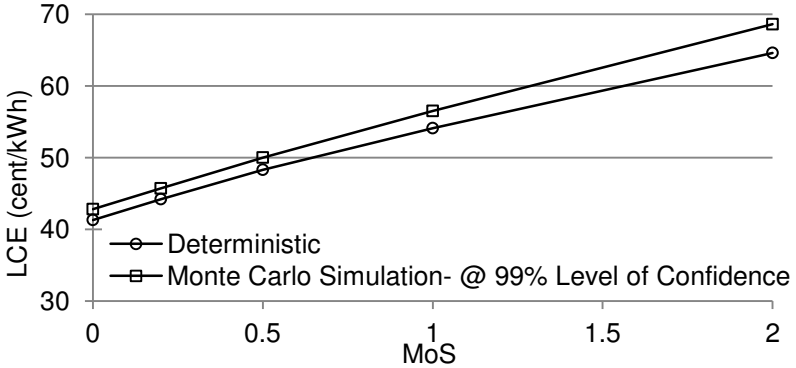

Figure 11-RD configuration: Levelised cost of energy calculated based on deterministic optimisation and the levelised cost of energy obtained by Monte Carlo simulation at 99% LOC.

5.3 Case Study 3: Wind-PV-Diesel-Battery Configuration

For different margins of safety the optimal size of the system components are obtained and shown in Table 8. The last row of this table includes the results of optimisation without using a margin of safety, where the size of the diesel generator and the battery bank are optimised along with the other design variables.

Figure 12 shows the system cost and LCE versus the margin of safety used in sizing the diesel generator. Comparing this figure with Figures 2 and 9, a different behaviour is observed. While in both RB and RD configurations the cost increases with safety factors ($T_a(1+\mathrm{MoS})$ and MoS), in the case of RBD configuration the cost initially reduces with the safety factor (MoS). It should be noted that in case of RD configuration, the nominal size of the diesel generator is determined based on the maximum hourly-averaged peak load, while in case of RBD configuration it is found based on the maximum daily-averaged load. This leads to smaller nominal sizes. Reduction in the cost as MoS (and consequently the size of the diesel generator) increases is due to (i) more usage of diesel as the source of power (which is more cost effective than the renewable resources) and (ii) less usage of the battery bank which leads to fewer and shallower discharges and consequently less replacement cost. Increase in the cost for MoS beyond a certain value is due to longer periods of time at which the generator does not operate at its nominal power (at its highest efficiency).

Table 8. RBD configuration: Results of the deterministic optimal design.

Design Case	Diesel generator sized based on MoS MoS(%)	Wind turbine rotor radius (m) [rated power (kW)]	PV panel area (m^2) [nominal pick power (kWp)]	No. of batteries	Diesel nominal power (kW)	Penetration (%)	TLSC ($)	LCE (cent/kWh)
D17	0	8.7 [94]	33 [2.8]	62	4.86	282	262,620	45.4
D18	20	4.7 [28]	89 [7.4]	40	5.84	116	255,180	43.2
D19	50	6.5 [53]	43 [3.6]	34	7.29	159	225,070	38.9
D20	100	6.0 [45]	10 [0.8]	34	9.73	119	210,519	36.4
D21	200	6.0 [45]	0 [0]	14	14.59	113	180,860	31.2
D22	500	5.0 [31]	0 [0]	28	29.18	76	199,460	34.5
D23	Diesel generator optimised for cost	6 [45]	0 [0]	14	14.0	113	179,980	31.1

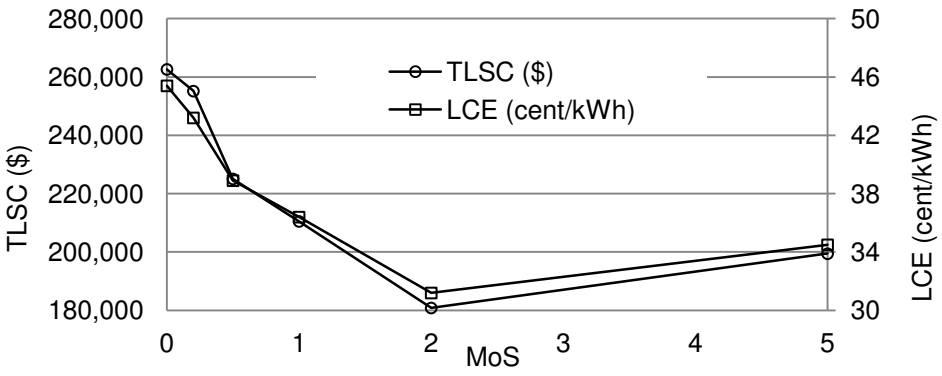

Figure 12-RBD configuration: Cost versus MoS .

Similar to Case Studies 1 and 2, for each design case, a Monte Carlo simulation is carried out to quantify the probability of failure of the system with respect to the system reliability measures as well as the cost obtained via the deterministic design method. The system performance characteristics at 99% LOC are also extracted from the results of the Monte Carlo simulation and are presented in Table 9.

Probability of failure of the system with respect to the expected reliability measures ($U_t = 0$, $BO_t = 0$ and $MTBF = 8760$ h) and cost ($C_l \le C_{l,det}$) versus MoS are shown in Figure 13. It can be observed that for lower MoS , irrespective of the value of MoS , high probability of failure in both the expected reliability and the cost are expected. As MoS increases, the probability of failure in the expected reliability measures reduces to zero. This is due to having a lower renewable penetration and more contribution of the diesel generator, as a reliable source, in generating power. In other words, the deterministic method can be used to design reliable RBD systems in terms of supplying the power if a suitable (large enough) MoS is used.

Table 9. RBD configuration: Probability of failure of design cases with respect to reliability and cost criteria.

Design Case	Probability of Failure (%)		System performance characteristics @ 99% LOC (PF=1%)					
	$U_t = 0$ $BO_t = 0$ $MTBF = 8760$	$C_l \le C_{l,det}$	BO_t (h)	BO_{max} (h)	BO_{av} (h)	U_t (kWh)	MTBF (h)	C_l (cent/kWh)
D17	100	100	93	2	1.4	96.6	123	46.4
D18	100	100	150	2	1.6	86.4	85	44.9
D19	100	100	67	2	1.2	44.0	142	40.3
D20	100	100	79	3	1.3	59.4	131	37.9
D21	96.2	100	9	1	1	1.3	1092	32.6
D22	0	100	0	0	0	0	8760	36.3
D23	99.5	100	12	1	1	2.6	787	32.4

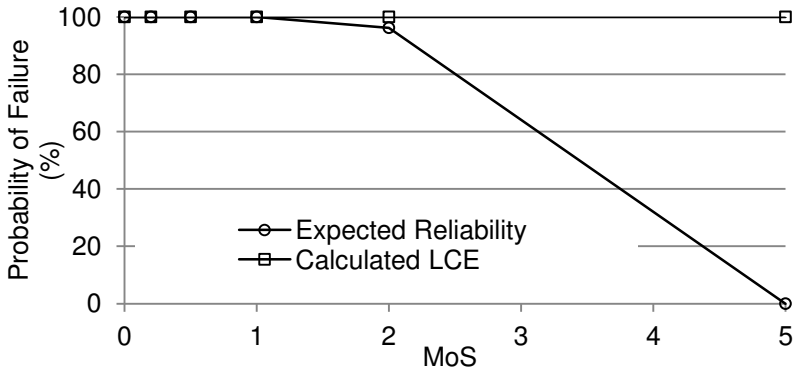

Figure 13-RBD configuration: Probability of failure of the system with respect to the expected reliability and cost criteria versus MoS .

The variation of reliability measures at 99% LOC versus MoS are shown in Figures 14 to 16. These figures show how the unpredictable fluctuating behaviour of the reliability measures at lower margins of safety (here, $MoS < 1$) becomes a predictable trend towards enhancing the reliability of the system at higher margins of safety (here, $MoS \geq 1$).

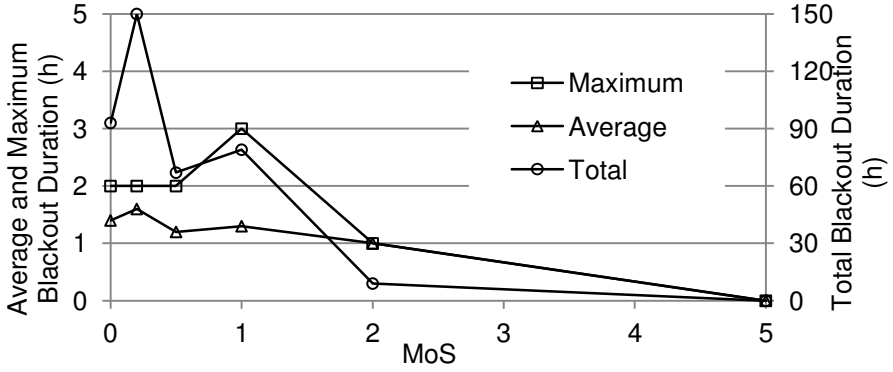

Figure 14-RBD configuration: Blackout duration at 99% LOC versus MoS .

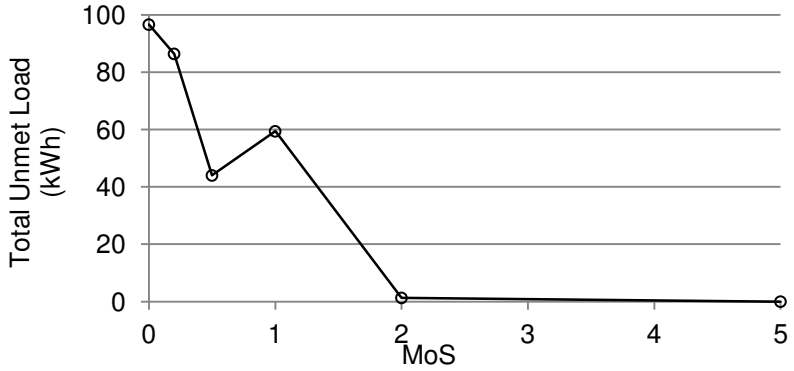

Figure 15-RBD configuration: Total unmet load at 99% LOC versus MoS

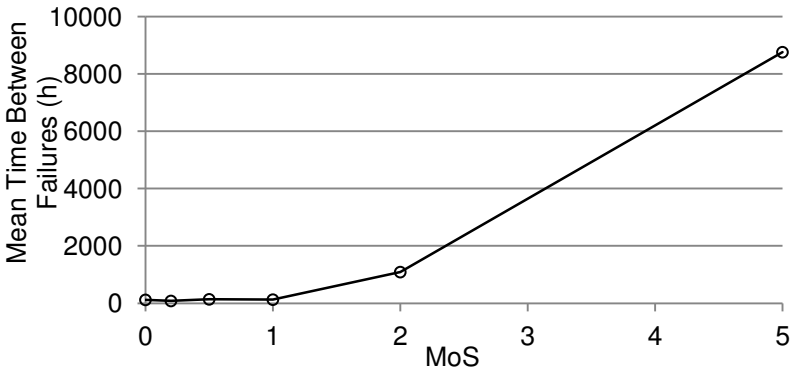

Figure 16-RBD configuration: MTBF at 99% LOC versus MoS

Figure 17 shows the solution space for designs D17 to D23 in LCE-total blackout duration plane, both calculated at a LOC of 99%. It can be observed that only designs D21 and D22 (with highest MoS) and D23 (optimised without using a margin of safety) are Pareto solutions. This highlights the importance of having a criterion to distinguish between low and high margins of safety in performing a reliable deterministic design.

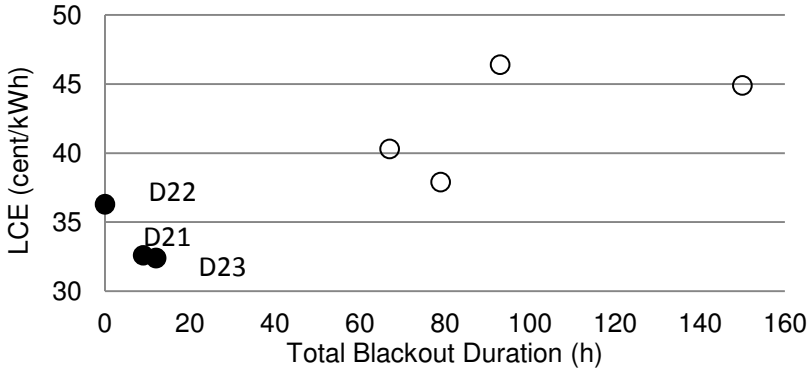

Figure 17-RBD configuration: Solution space for design cases D17 to D23.

Figure 18 compares LCE calculated deterministically with the LCE obtained via Monte Carlo simulation at a LOC of 99%. The deviation between the two curves becomes more significant as MoS (or equivalently the size of the diesel generator) increases. This shows that, as for the other two studied configurations, the results of deterministic optimisation for the objective of cost are not reliable for the RBD configuration.

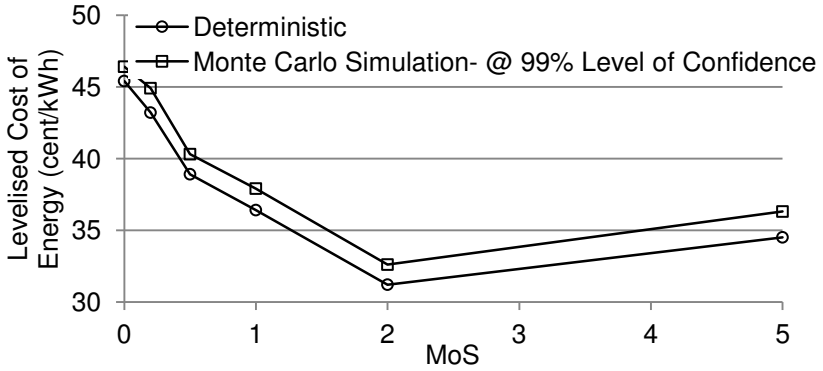

Figure 18-RBD configuration: Levelised cost of energy calculated based on deterministic optimisation and the levelised cost of energy obtained by Monte Carlo simulation at 99% LOC.

6 Summary and Conclusion

Size optimisation of standalone HRES is a multi-objective optimisation problem with two conflicting objectives of cost and reliability. Uncertainties in renewable resources and demand load affect the reliability of the system in supplying power whenever demanded. In deterministic design methods, the uncertainties in renewable resources and demand load are ignored; instead it is assumed that by employing safety factors and considering worst-case-scenarios, reliable systems can be designed. By doing this, the objective of reliability is eliminated from the original optimisation problem. The design problem reduces to a single-objective cost-driven optimisation. Generally, selection of safety factors is highly subjective, depending on the designer experience and judgment. In case of standalone HRES, the optimum safety factors, if there are any, depend on the renewable resources and load profile as well as the distribution and level of uncertainties.

In order to evaluate the reliability of deterministic design methods for three standalone HRES configurations (wind-PV-battery, wind-PV-diesel and wind-PV-battery-diesel), first, deterministic design methods are employed to find the optimal size of the system components for different values of safety factors. Then, for each design case, using Monte Carlo simulation ($n_{sim} = 10^5$), the effect of safety factors on reliability and cost of the system are investigated.

The probability calculated using Monte Carlo simulation has random errors due to limited sample size. To ensure the accuracy of the Monte Carlo simulation results, examining $n_{sim} = 10^6$ for two design cases D9 and D12, it was found that either the difference between the results is negligible (for D9) or the results are the same (for D12). Zero probability of failure for design D12 is due to the presence of diesel in the system configuration as well as using bounded uniform distribution for uncertainties.

In performing reliability analysis, the reliability measures unmet load, blackout durations (total, maximum and average) and mean time between failures are considered. Only few sources of uncertainties with uncertainties lower than the expected levels in practice are used to define conservative case studies in favour of deterministic methods. However, results show that deterministic methods fail to serve as reliable methods in sizing cost-effective and reliable systems. Exploiting the obtained results the following conclusions are drawn:

1. Calculated costs via a deterministic optimisation methods deviate from the costs obtained by employing Monte Carlo simulation even without having any uncertainty in the cost modelling. This deviation is due to the presence of uncertainties in power modelling, demand load and renewable resources which affect the replacement cost (batteries and diesel generator) and variable O&M cost (fuel consumption). This deviation becomes more significant as the size of the battery bank/diesel generator increases. Deviation between the cost calculated deterministically and the cost obtained using Monte Carlo simulation challenges the validity of the results of deterministic optimisation for the objective of cost.

RB configuration

2. The overall safety factor $T_a(1+\mathrm{MoS})$ has significant effect on the size of the battery bank and consequently the cost of the system. Both increase linearly with $T_a(1+\mathrm{MoS})$.

3. While parameters such as autonomy period and margin of safety used in deterministic designs are considered to have a direct influence on the reliability of the system, no predictable pattern representing the effect of these parameters on the reliability of the system could be found. This challenges the usability of these parameters in design of reliable systems of RB configuration.
4. Using large battery banks with charging efficiency of less than 100%, if not accompanied by the right size for renewable components, may lead to less reliable systems.
5. For this configuration, the results of deterministic optimisations are not trustworthy neither with respect to the reliability nor the cost of the system.

RD configuration

6. Similar to RB configuration, the system cost increases almost linearly with MoS .
7. In contrast to the RB configuration, parameter MoS used in deterministic design of RD configuration has a direct influence on the reliability of the system. That is, employing high-enough MoS leads to reliable systems in supplying power. However, as the cost of the system is directly proportional to the selected MoS , deterministic design methods cannot be used for multi-objective optimisation unless "high-enough" is quantified. For this configuration there exists an optimum value for MoS which cannot be quantified via deterministic methods, as it depends on the level and distribution of uncertainties. A procedure including both deterministic and probabilistic analyses is required to find MoS which corresponds to a desired reliability with minimal cost.

RBD configuration

8. Parameter MoS has a mix effect on the cost of the designed systems. There exists a MoS which minimises the cost and can be found via deterministic methods for a given site.
9. The reliability of the system shows little sensitivity to lower margins of safety. Higher margins of safety have direct influence on the reliability of the designed system. A high-enough MoS guarantees the reliability of the system in supplying power. Quantification of the MoS , which leads to a reliable system, or the border separating low and high margins of safety, cannot be carried out via deterministic methods as it depends on the distribution and level of uncertainties corresponding to renewable resources and demand load.

Using different values for the parameters defined in Table 2 would obviously lead to different optimal sizes and therefore different system costs. Using different values and forms for the uncertainties defined in Table 3 would lead to different values for the reliability measures. However, the general conclusions above, which are based on the results of conservative case studies, will be still valid. Incorporating more realistic uncertainties would obviously lead to similar conclusions, demanding the development of robust nondeterministic or hybrid deterministic/nondeterministic methods for sizing standalone HRES.

Appendix

Renewable Resources and Demand Load Profiles [28]

It is assumed that the wind speed measurement station elevation above the ground, h_{ref} in Equation (15), is 3 m. The demand load used in this study has the same profile as that of in [28] but it is scaled up by a factor of 3.

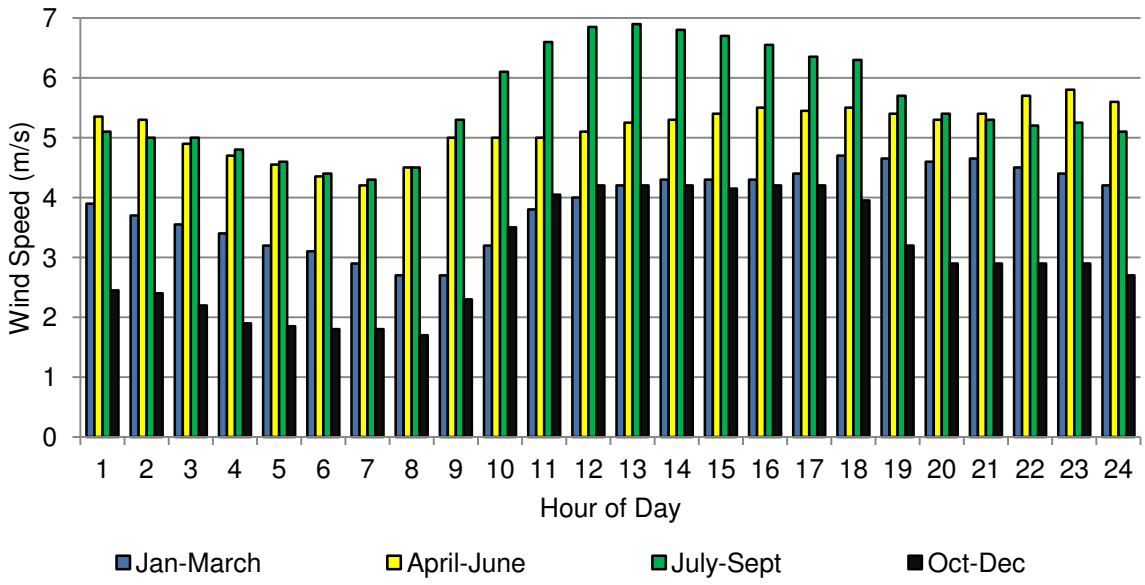

Figure A1-Seasonal hourly-averaged wind speed.

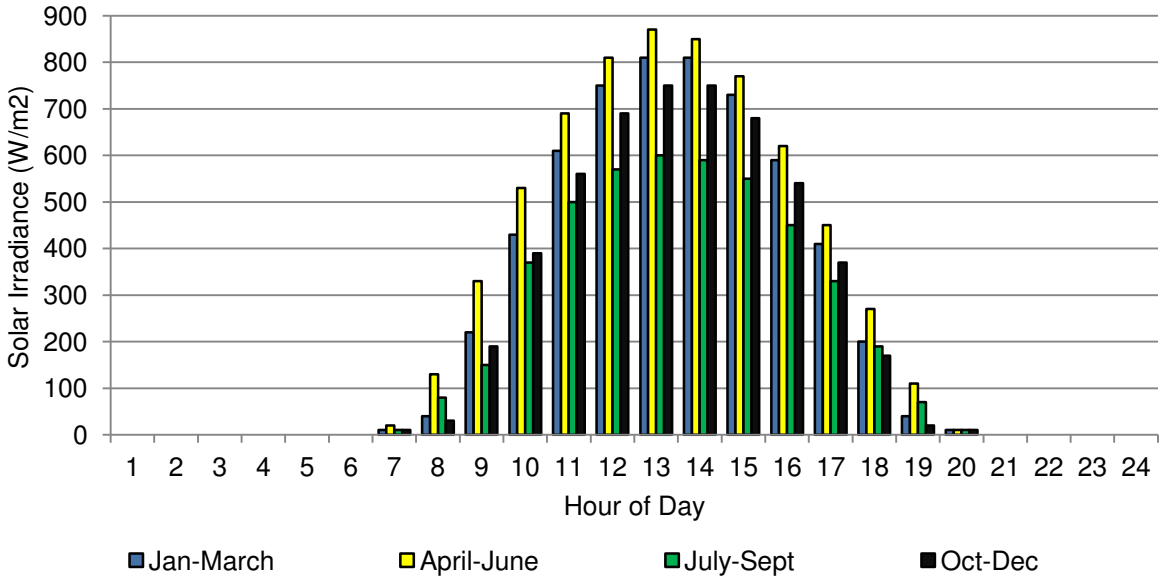

Figure A2-Seasonal hourly-averaged solar irradiance.

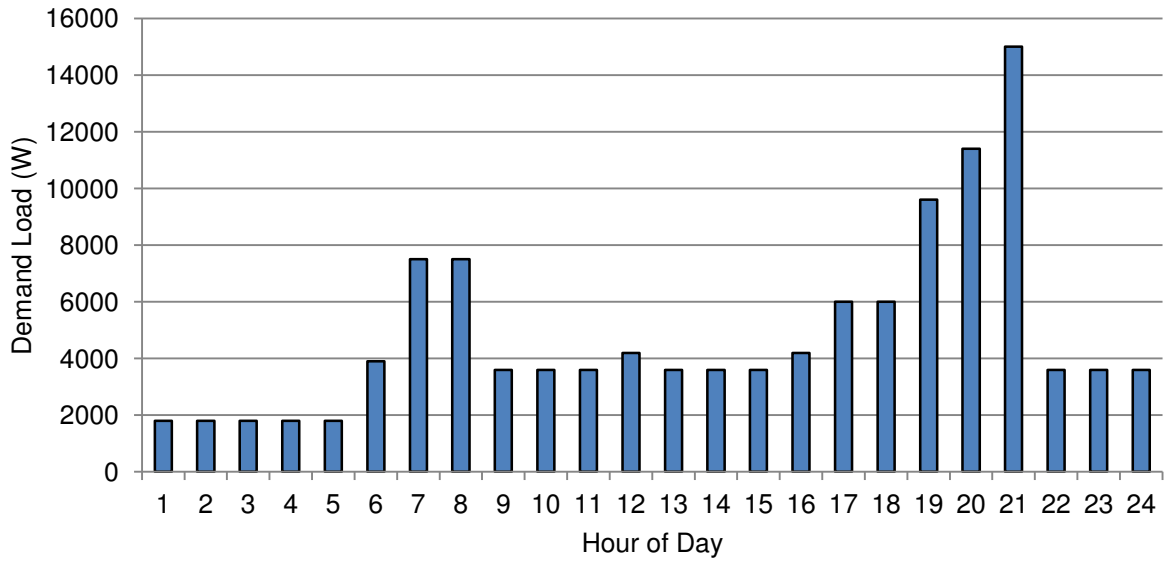

Figure A3-Hourly-averaged demand load.

Multiple polynomial regression in a least squares sense

Let N_{WT} be the number of observed wind turbines and N_V (the number of wind speeds between cut-in and cut-out velocities: $V=[V]_{1\times N_V}$) be the number of predictors at each of N_{WT} observations. In descending powers, the $q+1$ coefficients ($[C]_{(q+1)\times 1}$) of the q-order polynomial model:

$$C_P = C_1 V^q + C_2 V^{q-1} + \cdots + C_q V + C_{q+1} \tag{A.1}$$

can be obtained as:

$$[C]_{(q+1)\times 1} = \left(A^T A\right)^{-1} A^T B \tag{A.2}$$

in which:

$$B = \begin{bmatrix} \begin{bmatrix} C_{P_{1,1}} \\ \vdots \\ C_{P_{N_{WT},1}} \end{bmatrix}_{N_{WT}\times 1} \\ \vdots \\ \begin{bmatrix} C_{P_{1,N_V}} \\ \vdots \\ C_{P_{N_{WT},N_V}} \end{bmatrix}_{N_{WT}\times 1} \end{bmatrix}_{N_{WT}N_V\times 1} \tag{A.3}$$

where, $C_{P_{i,j}}$ is the power coefficient of the i-th wind turbine at the j-th wind speed, and A is defined as:

$$A=\begin{bmatrix} \begin{bmatrix} V_1^q & \cdots & V_1^0 \\ \vdots & \cdots & \vdots \\ V_1^q & \cdots & V_1^0 \end{bmatrix}_{N_{WT}\times(q+1)} \\ \vdots \\ \vdots \\ \vdots \\ \begin{bmatrix} V_{N_V}^q & \cdots & V_{N_V}^0 \\ \vdots & \cdots & \vdots \\ V_{N_V}^q & \cdots & V_{N_V}^0 \end{bmatrix}_{N_{WT}\times(q+1)} \end{bmatrix}_{N_V N_{WT}\times(q+1)} \quad \text{(A.4)}$$

References

[1] Turkay BE, Telli AY. Economic analysis of standalone and grid connected hybrid energy systems. Renewable Energy 2011;36:1931-43.

[2] Bajpai P, Dash V. Hybrid renewable energy systems for power generation in stand-alone applications: A review. Renewable and Sustainable Energy Reviews 2012;16:2926-39.

[3] Panayiotou G, Kalogirou S, Tassou S. Design and simulation of a PV and a PV-Wind standalone energy system to power a household application. Renewable Energy 2012;37:355-63.

[4] Shen WX. Optimally sizing of solar array and battery in a standalone photovoltaic system in Malaysia. Renewable Energy 2009;34:348-52.

[5] Ribeiro LA, Saavedra OR, Lima SL, et al. Making isolated renewable energy systems more reliable. Renewable Energy 2012;45:221-31.

[6] Dufo-Lopez R, Bernal-Agustin JL. Multi-objective design of PV-wind-diesel-hydrogen-battery systems. Renewable Energy 2008;33:2559-72.

[7] Bernal-Agustin JL, Dufo-Lopez R. Simulation and optimization of stand-alone hybrid renewable energy systems. Renewable and Sustainable Energy Reviews 2009;13:2111-8.

[8] Sreeraj ES, Chatterjee K, Bandyopadhyay S. Design of isolated renewable hybrid power systems. Solar Energy 2010;841124-36.

[9] Yang H, Zhou W, Lu L, et al. Optimal sizing method for stand-alone hybrid solar–wind system with LPSP technology by using genetic algorithm. Solar Energy 2008;82:354-67.

[10] Baniasad-Askari I, Ameri M. Optimal sizing of photovoltaic-battery power systems in a remote region in Kerman, Iran. Proceedings of the Institution of Mechanical Engineers, Part A: Journal of Power and Energy 2009;223:563-70.

[11] Roy A, Kedare SB, Bandyopadhyay S. Physical design space for isolated wind-battery system incorporating resource uncertainty. Proceedings of the Institution of Mechanical Engineers, Part A: Journal of Power and Energy 2011;225:421-42.

[12] Roy A, Kedare SB, Bandyopadhyay S. Optimum sizing of wind-battery systems incorporating resource uncertainty. Applied Energy 2012;87:2712-27.

[13] Val DV, Chernin L, Yurchenko DV. Reliability analysis of rotor blades of tidal stream turbines. J Reliability Engineering & System Safety 2014;121: 26-33.

[14] Zhang CW, Zhang T, Chen N, Jin T. Reliability modeling and analysis for a novel design of modular converter system of wind turbines. J Reliability Engineering & System Safety 2013;111: 86-94.
[15] Nielsen JJ, Sørensen JD. On risk-based operation and maintenance of offshore wind turbine components. J Reliability Engineering & System Safety 2011;96:218-29.
[16] Kostandyan EE, Sørensen JD. Physics of failure as a basis for solder elements reliability assessment in wind turbines. J Reliability Engineering & System Safety 2012;108:100-7.
[17] Li YF, Zio E. A multi-state model for the reliability assessment of a distributed generation system via universal generating function. J Reliability Engineering & System Safety 2012;106:28-36.
[18] Taflanidis AA, Loukogeorgaki E, Angelides DC. Offshore wind turbine risk quantification/ evaluation under extreme environmental conditions. J Reliability Engineering & System Safety 2013;115:19-32.
[19] Perez-Canto S, Rubio-Romero JC. A model for the preventive maintenance scheduling of power plants including wind farms. J Reliability Engineering & System Safety 2013;119: 67-75.
[20] Kaabeche A, Belhamel M, Ibtiouen R. Sizing optimization of grid-independent hybrid photovoltaic/wind power generation system. Energy 2011;36:1214-22.
[21] Belfkira R, Zhang L, Barakat G. Optimal sizing study of hybrid wind/PV/diesel power generation unit. Solar Energy 2011;85:100-10.
[22] Burton T, Jenkins N, Sharpe D, Bossanyi E. Wind Energy Handbook, Second Edition, Wiley, 2011.
[23] Skarstein O, Uhlen K. Design considerations with respect to long-term diesel saving in wind/diesel plants. Wind Engineering 1989;13:72-87.
[24] Ashari M, Nayar CV. An optimum dispatch strategy using set points for a photovoltaic (PV)-diesel-battery hybrid power system. Solar Energy 1999;66:1-9.
[25] Short W, Packey DJ, Holt T. A Manual for the Economic Evaluation of Energy Efficiency and Renewable Energy Technologies, NREL/TP-462-5173, March 1995.
[26] Messac A, Chowdhury S, Zhang J. Characterizing and mitigating the wind resource-based uncertainty in farm performance. Turbulence 2012;13:1-26.
[27] Mani M, Pillai R. Impact of dust on solar photovoltaic (PV) performance: Research status, challenges and recommendations. Renewable and Sustainable Energy Reviews 2010;14:3124-31.
[28] Katti PK, Khedkar MK. Alternative energy facilities based on site matching and generation unit sizing for remote area power supply. Renewable Energy 2007;32:1346-62.

Nomenclature

A	Area (m^2)
BO	Blackout duration
C	Cost ($)
C_u	Unit cost ($/unit)
c	Battery capacity (Ah)
DOD	Depth of discharge (-)
d	Discount rate (-)
FR	Failure rate (-)
h_c	Ground-blade tip clearance (m)
i	Inflation rate (-)
I	Solar irradiance (W/m^2)
L	Demand load (W)
LLP	Loss of load probability (-)

MoS	Margin of safety
MTBF	Mean time to failure
N	Nominal life-span (years; hours of operation)
n	Number
n_B	Number of batteries in battery bank
n_d	Number of battery discharges per year
n_p	Number of performance measures
n_u	Number of uncertain parameter
P	Power (W)
PF	Probability of failure (-)
S	Size (various units)
SOC	State of charge (-)
T	Period of time
T_a	Autonomy period (days)
U	Unmet load (-)
U_t	Total unmet load (Wh)
UCRF	Uniform capital recovery factor
V_B	Battery bank voltage (V)
w	Penetration (-)
z_0	Site surface roughness (m)
α	Cost as a fraction of initial cost (-)
η_{PV}	Overall PV unit efficiency (-)
δ	Self-discharge rate (-); Variation range of uncertain parameters with uniform distribution (-)
ρ	Air density (kg/m^3)
η_{EG}	Wind turbine electrical and gearbox efficiency (-)

Subscripts

a	Autonomy; Available; Usable available; Annualised
av	Average
B	Battery
c	Capital
comp	HRES component (WT, PV, B, D)
D	Diesel
d	Daily
design	Design
e	Extractable
F	Fixed
fail	Failure
fc	Fully charged
h	Hourly
hub	Hub elevation
ins	Installation
max	Maximum
min	Minimum

nom	Nominal
O & M	Operation and maintenance
PV	Photovoltaic
p	Performance measures
R	Renewable
r	Replacement
real	Real
S	System
sim	Simulation
t	Total; Time
u	Unit, Uncertain parameter
V	Variable
WT	Wind turbine
y	Yearly

Symbols

$\overline{\varphi}_{\mathrm{T}}$	Averaged value of quantity φ over time period T
$\tilde{\varphi}$	Mean value of uncertain parameter φ
$\hat{\varphi}$	Random part of uncertain parameter φ

Abbreviations

HRES	Hybrid renewable energy system
LCE	Levelised cost of energy
LOC	Level of confidence
O&M	Operating and maintenance
RB	Renewable-battery
RD	Renewable-diesel
RBD	Renewable-battery-diesel
TLSC	Total life-span cost

List of Figures

List of Tables